AIP | Applied Physics Letters

Enhanced light extraction in organic light-emitting devices: Using conductive low-index layers and micropatterned indium tin oxide electrodes with optimal taper angle

Jungmin Choi, Tae-Wook Koh, Soohyun Lee, and Seunghyup Yoo

Citation: Applied Physics Letters **100**, 233303 (2012); doi: 10.1063/1.4724306
View online: http://dx.doi.org/10.1063/1.4724306
View Table of Contents: http://scitation.aip.org/content/aip/journal/apl/100/23?ver=pdfcov
Published by the AIP Publishing

Enhanced light extraction in organic light-emitting devices: Using conductive low-index layers and micropatterned indium tin oxide electrodes with optimal taper angle

Jungmin Choi, Tae-Wook Koh, Soohyun Lee, and Seunghyup Yoo[a)]
Department of Electrical Engineering, Korea Advanced Institute of Science and Technology (KAIST), Daejeon 305-701, South Korea

(Received 20 March 2012; accepted 16 May 2012; published online 5 June 2012)

We present our study on organic light-emitting diodes (OLEDs) in which outcoupling is enhanced based on a bilayer electrode consisting of a conductive low-index layer and micro-patterned indium tin oxide (ITO) layers. Optical simulation reveals that the taper angle of an ITO pattern is among the most critical parameters influencing the outcoupling efficiency in the proposed structure. A fabrication method based on a lift-off process is then employed to control the taper angle of the ITO pattern to be in the optimal range. OLEDs with the proposed electrode structure exhibit 50%–70% enhancement in external quantum efficiency over reference devices. © *2012 American Institute of Physics*. [http://dx.doi.org/10.1063/1.4724306]

Organic light-emitting diodes (OLEDs) have entered the mobile display market, one of the fastest growing segments of the display industry, as an ideal light source with various attractive characteristics. In addition, they are expected to play a significant role also in the lighting industry in a near future. In both fields of applications, the importance of efficiency improvement cannot be overemphasized as the enhanced efficiency not only offers a high lumen per unit cost but also enables a lower operating current density, which then tends to extend the device lifetime and reduce the overall cost of ownership. The efficiency of most OLEDs, however, is ultimately limited by relatively low outcoupling efficiency (η_{out})—the ratio of the number of the extracted photons to that of the internally generated photons—while a careful device engineering can lead to an internal quantum efficiency (IQE) of almost 100%.[1,2] The limited outcoupling results from the stratified geometry inherent to an OLED, which causes total internal reflections at its glass/indium tin oxide (ITO) and air/glass interfaces. Outcoupling efficiency is known to be limited typically to 20% or less, although the exact number can vary depending on a model and assumptions used therein.[3–5] Some of the photons that cannot be coupled out are simply lost by absorption or plasmonic coupling, but others are trapped or guided within a substrate [substrate-confined (SC) mode] or within ITO/organic layers [waveguide (WG) mode].[4] The portion of these SC and WG modes can range from 20% to as much as 60% even when loss due to absorption and surface-plasmonic loss is taken into account.[4] Hence, extraction of those SC and WG modes, if possible, can provide an opportunity to enhance the external quantum efficiency (EQE) of an OLED to a significant degree.

Many groups have thus tried to develop a device architecture that can convert SC and/or WG modes into outcoupled modes.[6–9] To this end, we recently reported on the outcoupling enhancement in OLEDs employing a bilayer anode, consisting of a conductive low-index layer (CLIL) covering a micro-patterned ITO electrode, the pattern of which repeats in a 2D square array with a spatial period of several micrometers.[10] It was demonstrated that the proposed structure can effectively extract WG modes while having the advantages of (i) spectrally neutral enhancement; (ii) little or no distortion of angular characteristics; (iii) no optical blurring; and (iv) absence of an electrically inactive area, all of which are the characteristics that are highly desired for practical applications yet have rarely been realized simultaneously. Nevertheless, the relative enhancement in our previous work was rather limited at approximately 25%. In this study, we investigate how one can take a full advantage of what the proposed CLIL-based structure can offer in enhancing η_{out} of OLEDs. We first perform an optical simulation while varying several parameters to reveal the most important factor(s) for WG-mode extraction. Upon identification of key parameter(s), we then present a simple method that can lead to a further significant enhancement in η_{out} in CLIL-based OLEDs.

Figures 1(a) and 1(b) present a schematic top view of the anode structure under study and a cross-sectional view of an OLED made thereof, respectively. A unit cell (a region surrounded with a solid line in Fig. 1(a)), which consists of (i) a square-shaped $d \times d$ region only with poly(3,4-ethylenedioxythiophene): poly(styrene sulfonate) (PEDOT:PSS) (=region P) and (ii) a region with both ITO and PEDOT:PSS (=region I/P), repeats with a spatial period of a either in a square or hexagonal lattice configuration. When the proposed anode is used in OLEDs, the light travelling laterally within organic layers, which corresponds to WG modes, eventually runs against the edge of the ITO micro-patterns that have an inclined surface covered with PEDOT:PSS. Some of those lights can change their travelling directions in such a way that they are eventually outcoupled. The ray diagrams in Fig. 1(b) show the three representative cases in which WG modes are converted to outcoupled modes in the proposed device structure.[10] Note that both of the rays originating from region P (the rays represented by solid and

[a)]Author to whom correspondence should be addressed. Electronic mail: syoo.ee@kaist.edu. Telephone: +82-42-350-3483. Fax: +82-42-350-8083.

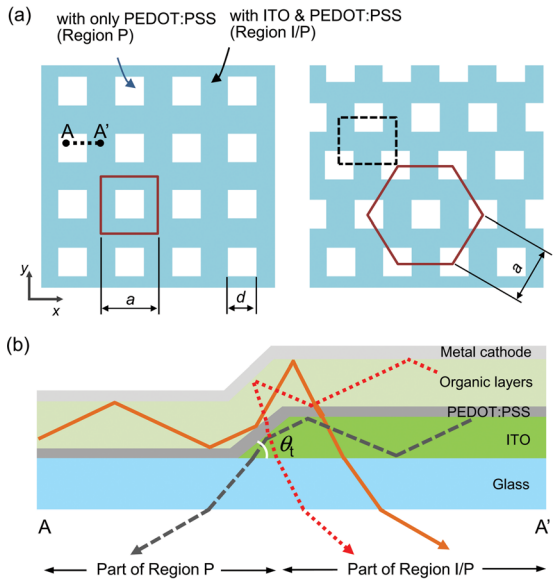

FIG. 1. (a) Top-view diagram of the bilayer anode structures under study (left: square lattice; right: hexagonal lattice) and (b) cross-sectional diagram (along the line A-A′) of an OLED containing them. Three representative ray diagrams are shown to illustrate the working principle of the proposed structure.

dashed lines) and region I/P (the ray represented by dotted lines) can be converted to outcoupled modes. For clarification, the ray represented by the dashed line in Fig. 1(b) corresponds to the case in which the light initially generated in region P on the other side (not shown here) enters into the ITO layer in region I/P through the inclined surface and is guided therein.[10] It should be noted that extraction of WG modes in all the cases shown above is enabled by the index contrast provided by PEDOT:PSS, which has a lower refractive index (1.4–1.6)[11] than those of ITO and organic layers (1.7–2.0), allowing the micro-structuring to have a significant optical effect.

To see how we can further improve η_{out} in the proposed structure, we carried out an optical simulation using commercial illumination-optic software (LightTools^{TM}), which is based on geometrical and statistical optics. Simulation was done at a wavelength of 550 nm while the following parameters were varied: the taper angle (θ_t) of the inclined surface (Fig. 1(b)), the lattice geometry (square vs. hexagonal), the spatial period a, and the ratio of d to a. The effect of absorption occurring within ITO and organic layers was also investigated and included when studying the effects of a and d/a ratio. This modification is essential in simulating a more realistic situation and thus minimizing the possible overestimation because some of the waveguide light may need to travel over a few to several micrometers before being converted to outcoupled modes in the proposed structure.

The simulation results are summarized in Figs. 2(a)–2(d). First of all, it is noted that the taper angle (θ_t) is among the most critical parameters influencing η_{out} in the proposed device geometry and that the optimum taper angle ($\theta_t^{(opt)}$) is approximately $45 \pm 10°$ in all of the cases we simulated. If θ_t is too small, a ray that could otherwise be outcoupled will continue to be guided as if nothing significant happens near the tapered interface and will eventually be lost by absorption. Likewise, if θ_t is too high, the same ray of light would not reflect from the inclined interface as efficiently as in the optimal case because it no longer meets the total internal reflection condition. Hexagonal lattice geometry is also shown to be helpful, albeit not as significant

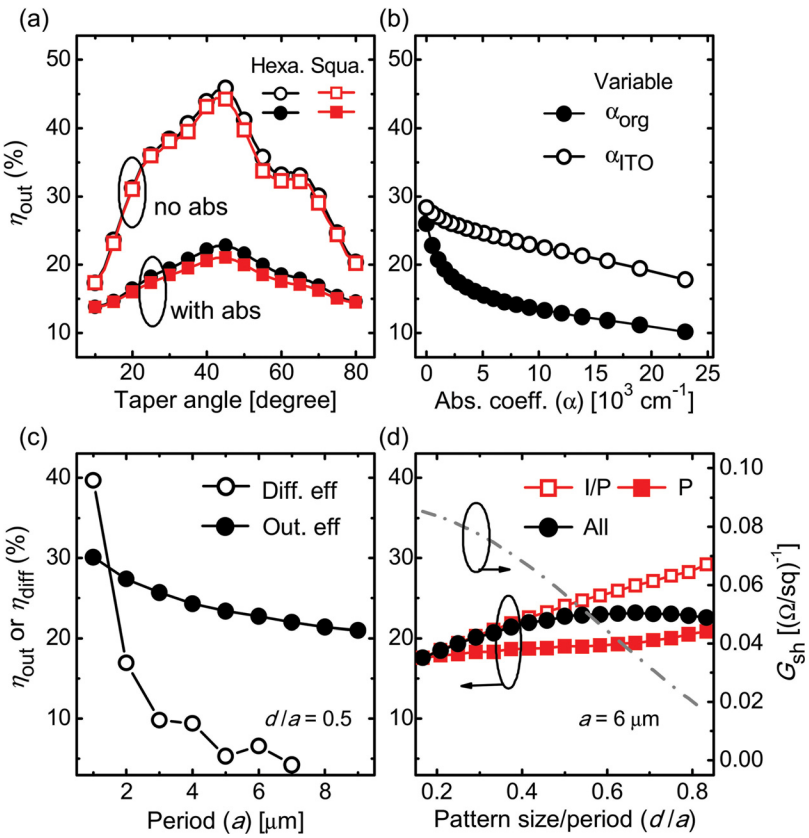

FIG. 2. Optical simulation results for OLEDs with the proposed anode structure: (a) η_{out} vs. taper angle (θ_t) for square and hexagonal lattice geometries with or without absorption from ITO or organic layers assumed; (b) η_{out} vs. absorption coefficient of ITO (α_{ITO}) or organic (α_{org}) layers; (c) η_{out} vs. spatial period (a) with d/a of 0.5. Also shown is the curve for diffraction efficiency (η_{diff}) vs. a. (1D grating assumed for simplicity.); (d) η_{out} vs. d/a with a of 6 μm. Separate contributions of the light originating from region P and region I/P, respectively, are also shown. The following assumptions were used in (a)-(d) unless specified otherwise $\theta_t = 45°$; hexagonal lattice ($a = 6\,\mu m$, $d/a = 0.5$); $\alpha_{ITO} = 1.1 \times 10^4\,cm^{-1}$; and $\alpha_{org} = 1.0 \times 10^3\,cm^{-1}$.

as θ_t, in improving η_{out}. This is because hexagonal lattice geometry packs slightly more structured interfaces within a given area than square lattice geometry does, increasing the overall probability that the light will run across the inclined surface of the micro-patterns, which is the key interface enabling the enhanced extraction. The graphs shown in Figs. 2(b)–2(d) and all the experimental results are thus given for hexagonal lattice geometry unless specified otherwise.

The estimated value for η_{out} exhibited a significant drop when possible absorption in organic and/or ITO layers was taken into account, as can be seen from Figs. 2(a) and 2(b). While absorption in both organic and ITO layers had a significant influence on η_{out}, absorption occurring in organic layers was shown to be particularly critical. This is partly because the cases in which the rays are guided mainly along organic layers (rays represented by solid and dotted lines) are more abundant than the other case in the proposed structure.

It may be stressed from the results observed in Fig. 2(b) that any optical structure extracting WG modes should be able to convert them into outcoupled modes before the rays travel too far or preferably within a characteristic distance of $1/\alpha$, which is 10 μm and 1 μm for α of $10^3\,\mathrm{cm}^{-1}$ and $10^4\,\mathrm{cm}^{-1}$, respectively. In fact, the implication of such absorption effect can be readily seen from Fig. 2(c) presenting the curve of η_{out} vs. a. With α of organic ($=\alpha_{org}$) and ITO layers ($=\alpha_{ITO}$) assumed at reasonable values of $10^3\,\mathrm{cm}^{-1}$ and $1.1\times10^4\,\mathrm{cm}^{-1}$,[12–14] respectively, η_{out} increases from 22.7% to 30.1% as a decreases from 7 μm to 1 μm when θ_t and d/a are fixed at 45° and 0.5. Nevertheless, one may not decrease a to an arbitrarily small value as it can incur problems in other aspects. If a is below 2–4 μm, the minimum feature size for d can be too small to be considered reasonable in terms of fabrication cost. Moreover, undesirable wavelength dependence may occur if a is too small. Diffraction phenomenon is one example. A significant diffraction effect, if any, will induce an undesirable rainbow-like feature when an OLED device is viewed under ambient light. The curve with open circles in Fig. 2(c) presents the calculated results of diffraction efficiency (η_{diff}) obtained with Diffract-MOD™ as a function of a for ambient light reflecting from the proposed OLED device. For simplification, the unit cell used in calculation of η_{diff} was given by the one shown in the square lattice of Fig. 1(a) in the x-direction and has a full OLED structure but elongated to an infinite scale in the y-direction so that the model system can be treated as a 1D reflection grating. The result indicates that η_{diff} for the reflected light is relatively large unless a becomes larger than 4 μm. From the observations discussed in this paragraph, one may regard 5–7 μm as an optimal spatial period in the proposed system.

The effect of the "d/a"-ratio turns out to be rather subtle. Note that the travel distance to the inclined interface becomes shorter (longer) for light originating from region I/P (region P) as d/a increases for a fixed a. Hence, the partial outcoupling efficiency for the light generated from region I/P ($=\eta_{out}^{(I/P)}$) tends to increase as d/a increases, while that for the light generated from region P ($=\eta_{out}^{(P)}$) tends to decrease. Since overall η_{out} is determined by the area-weighted average of $\eta_{out}^{(I/P)}$ and $\eta_{out}^{(P)}$, the competition between those two components results in η_{out} that increases with d/a at first but saturates after d/a becomes larger than about 0.5. Note that the effective sheet resistance $R_{sh}^{(eff)}$ of the proposed bilayer electrode tends to increase with d/a due to an increase in the relative portion of region P, which has a higher sheet resistance than region I/P. In a hexagonal lattice, $R_{sh}^{(eff)}$ can be obtained, upon consideration of its symmetry, by calculating the resistance over the rectangular area surrounded by the dashed line in Fig. 1(a) and correcting it for its aspect ratio. In this way, $R_{sh}^{(eff)}$ of the proposed bilayer anode in a hexagonal lattice geometry is given by

$$R_{sh}^{(eff)}=\frac{2}{\sqrt{3}}\left[R_{sh}^{(ITO)}\left(\frac{\sqrt{3}}{2}-\frac{d}{a}\right)+R_{sh}^{(PED)}\left(1+\frac{a-d}{d}\frac{R_{sh}^{(PED)}}{R_{sh}^{(ITO)}}\right)^{-1}\right]. \quad (1)$$

The sheet conductance ($=G_{sh}^{(eff)}=1/R_{sh}^{(eff)}$) is shown in Fig. 2(d) for the case in which $R_{sh}^{(ITO)}=11\ \Omega/\mathrm{sq}$ and $R_{sh}^{(PEDOT)}=683\ \Omega/\mathrm{sq}$.[10] As long as d/a is smaller than 0.56, $R_{sh}^{(eff)}$ is maintained within 20 Ω/sq. From the observed trend of η_{out} and $G_{sh}^{(eff)}$ over d/a, the optimal d/a ratio considering both electrical and optical properties may be set at around 0.5.

Based on the results obtained from the theoretical study, we narrowed down to the hexagonal lattice geometry with a and d/a set to 6 μm and 0.5, respectively. Then, we focused our efforts on controlling θ_t to be in the optimal range considering its strong potential to enhance η_{out}. It should be noted that controlling the taper angle is not a trivial task. In the wet-etching process commonly used for ITO etching, in particular, it is challenging to control the edge shape of ITO patterns due to its isotropic etching character.[15] According to our previous results,[10] the ITO pattern produced with such wet-etching process resulted in θ_t of approximately 25° or less, which is much smaller than $\theta_t^{(opt)}$. Therefore, we adopted the lift-off process outlined in Fig. 3(a), in which the taper angle control was done using a commercially available negative photoresist (AZ5214, AZ Electronic Materials).

Note that the exposure process shown as a single step for simplicity in Fig. 3(a) in fact consists of multiple steps

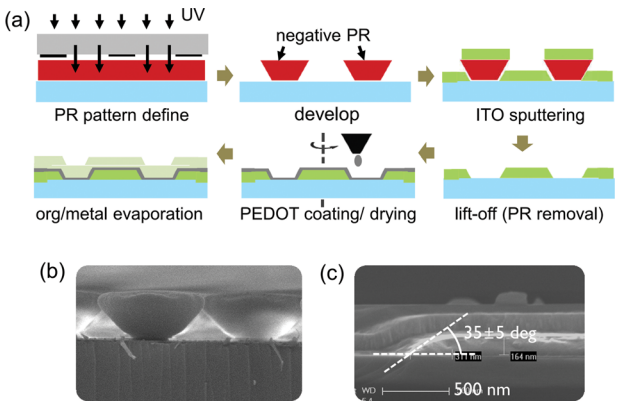

FIG. 3. (a) Overall process flow for fabrication of OLEDs based on the proposed anode structure of which the ITO pattern edge has the optimal taper angle. (b) The cross-sectional SEM images of the inverse trapezoidal structure created with negative photoresist (PR) and (c) that of the sputtered ITO pattern defined by the proposed lift-off process.

involving (i) spin-coating of AZ5214 on a precleaned substrate (4000 rpm, 30 s); (ii) pre-baking on a hotplate at 120 °C for 1 min; (iii) UV exposure using a mask aligner (Lithotech, ADE-100; i-line, 18.9 mW/cm^2) with a photomask in position; (iv) baking on a hotplate at 120 °C for 2 min; and (v) UV-exposure without the photomask under the same condition as (iii). Such multiple steps are common when AZ5214 is used as a negative/image-reversal resist. This is based on the fact that AZ5214 is a positive photoresist *as-is* but its UV-exposed part can be selectively activated and cross-linked when going through a proper heat treatment (110 °C–130 °C), as in the steps (iii)-(iv).[16] To obtain the pattern shapes with a desired inverse-trapezoidal structure having the proper range of taper angle, we carefully adjusted the exposure time. The optimized exposure time was 2 s and 30 s for the first and second exposure steps, respectively. It turned out that developing time was also influential. In general, a shorter developing time tended to yield a structure with a steeper slope (larger taper angle) because the developer solution has a relatively small amount of time to penetrate into the resist film. The optimized developing time was 30 s for the developer used in this work (AZ300MIF, AZ Electronic Materials).

Through the controlled process described above, we were able to obtain an inverse trapezoidal structure with the taper angle in the range of 30°–50° as shown in the scanning electron microscopy (SEM) image presented in Fig. 3(b). Then, an ITO layer with a thickness of 155 ± 10 nm was deposited by RF magnetron sputtering and subsequently went through the lift-off process using photoresist remover (AZ400T, AZ Electronic Materials). The taper angle of the final ITO pattern was measured to be 35 ± 5° (Fig. 3(c)), thanks to the good step coverage typical of the sputtering process. The average sheet resistance of the sputtered ITO layer was 35 Ω/sq, higher than that of commercial ITO electrodes, which is typically in the range of 10–15Ω/sq. After definition of ITO patterns, OLED devices were fabricated as described previously[10] with high-conductivity grade of PEDOT:PSS (Baytron PH 500, Clevios^{TM}) mixed with 5% dimethylsulfoxide (DMSO). The OLED devices were based on an archetypal heterojunction consisting of a hole transport layer (HTL) of N,N′-Bis(naphthalen-1-yl)-N,N′-bis(phenyl)-benzidine (NPB) and an electron transport/emission layer (ETL/EML) of tris(8-hydroxy-quinolinato) aluminum (Alq_3). The part of the PEDOT:PSS layer covering the outside of an active area was masked with an insulating layer to avoid the possibility of overestimation.

Figures 4(a) and 4(b) present the EQE and power efficiencies (PEs), respectively, of the OLED devices fabricated in this work as a function of luminance (L). In the high brightness range where the enhancement results predominantly from the optical effect,[10] the relative enhancement in EQE with respect to that of a reference device (planar; without PEDOT:PSS) was as large as 50%–70%. Their PE also showed the similar level of enhancement in the high L range. These results correspond to >2× improvement over the previous work,[10] which was based on the same CLIL-based devices with their ITO patterns defined by the wet-etching process. Since η_{out} of a reference OLED device ($\eta_{out}^{(ref)}$) is estimated to be 14.0% with absorption in ITO and organic

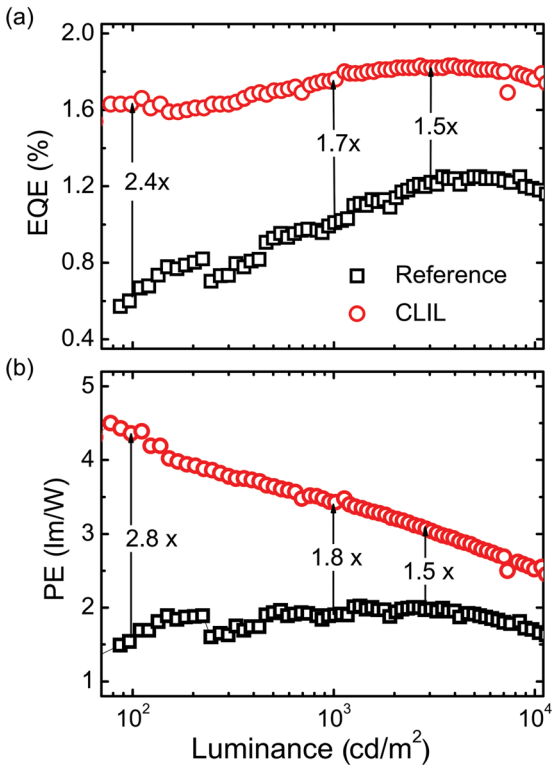

FIG. 4. Experimental results for (a) EQE and (b) PE vs. luminance of OLEDs under study. OLED devices are in the structure of glass/*x*/NPB (50 nm)/Alq_3 (50 nm)/LiF (1 nm)/Al with x being (i) planar ITO without PEDOT:PSS (="reference") or (ii) patterned ITO covered with PEDOT:PSS (="CLIL").

layers included, the estimated *optical* enhancement ratio of η_{out} for θ_t of 45 ± 10° is expected to be in the range of 1.43–1.63 and agrees well with the experimental result. Without inclusion of absorption effect, the maximum enhancement ratio over $\eta_{out}^{(ref)}$ (=17.6%) is estimated for θ_t of 45 ± 10° to be 2.03–2.61, which is too far from the experimental results; this reconfirms the importance of including the effect of absorption in predicting the η_{out} enhancement without severe overestimation. In the low brightness level, even a larger degree of enhancement was observed in both EQE and PE. For example, their EQE and PE were enhanced by 140% and 180%, respectively, at L of 100 cd/m^2. Such large enhancement in this brightness range is attributed not only to the optical benefit of the proposed structure but also to the electrical carrier balance improved by PEDOT:PSS.[10,17]

It is also noteworthy that the proposed process results in a relatively steep inclined surface, yet the edge is still smooth enough not to cause electrical shorts. Another type of process such as a directional, plasma-based dry-etching process[15] may also be considered, but one has to make sure that the employed method does not result in excessively sharp or rough edges that can make devices vulnerable to electrical shorts.

In summary, we have shown that the outcoupling enhancement due to the optical effect of a conductive index layer and micropatterned ITO electrodes can be improved to a value as high as 50%–70%. The taper angle increased close to the optimal range of approximately 45 ± 10° by the proposed lift-off process was a key to more than 2×

enhancement over the previous work, which was based on the equivalent structure but with the ITO patterns having smaller taper angles due to the limitation of the wet-etching process. Given the advantages of the CLIL-based method such as spectrally neutral enhancement, no angular distortion, absence of inactive area, and blur-free operation,[10] the proposed method is expected to play a significant role as an attractive method to enhance the efficiency of OLEDs in various applications.

This research was supported in part by Samsung Mobile Display (SMD) through the SMD KAIST OLED Research Center Program, by the National Research Foundation of Korea (NRF) grant funded by the Korea government (MEST) (No. 20120000815), and by the Human Resource Training Project for Strategic Technology funded by the Korea Institute for Advancement of Technology.

[1]C. Adachi, M. A. Baldo, M. E. Thompson, and S. R. Forrest, J. Appl. Phys. **90**, 5048 (2001).
[2]Y. Sun, N. C. Giebink, H. Kanno1, B. Ma, M. E. Thompson, and S. R. Forrest, Nature **440**, 908 (2006).
[3]J. Kim, P. K. H. Ho, N. C. Greenham, and R. H. Friend, J. Appl. Phys. **88**, 1073 (2000).
[4]R. Meerheim, M. Furno, S. Hofmann, B. Lüssem, and K. Leo, Appl. Phys. Lett. **97**, 253305 (2010).
[5]S.-Y. Kim and J.-J. Kim, Org. Electron. **11**, 1010 (2010).
[6]Y. Sun and S. R. Forrest, Nat. Photonics **2**, 483 (2008).
[7]W. H. Koo, S. M. Jeong, F. Araoka, K. Ishikawa, S. Nishimura, T. Toyooka, and H. Takezoe, Nat. Photonics **4**, 222 (2010).
[8]S. Reineke, F. Lindner, G. Schwartz, N. Seidler, K. Walzer, B. Lüssem, and K. Leo, Nature **459**, 234 (2009).
[9]K. Hong and J.-L. Lee, Electron. Mater. Lett. **7**, 77 (2011).
[10]T.-W. Koh, J. Choi, S. Lee, and S. Yoo, Adv. Mater. **22**, 1849 (2010).
[11]K. Fehse, K. Walzer, K. Leo, W. Lövenich, and A. Elschner, Adv. Mater. **19**, 441 (2007).
[12]J. S. Kim, P. K. H. Ho, D. S. Thomas, R. H. Friend, F. Cacialli, G. W. Bao, and S. F. Y. Li, Chem. Phys. Lett. **315**, 307 (1999).
[13]D. Z. Garbuzov, V. B. Bulović, P. E. Burrows, and S. R. Forrest, Chem. Phys. Lett. **249**, 433 (1996).
[14]T. Gerfin, and M. Grätzel, J. Appl. Phys. **79**, 1729 (1996); also see SOPRA n&k database.
[15]S. Franssila, *Introduction to Microfabrication* (Wiley, West Sussex, UK, 2004), Chap. 11.
[16]Product data sheet, *AZ 5214E Image Reversal Photoresist*, Clariant Corp, Somerville, NJ, 1990.
[17]There is also an electrical artifact due to a noise being amplified when $L < 100$–200 cd/m^2.